

# An investigation on the mortars containing blended cement subjected to elevated temperatures using Artificial Neural Network (ANN) models

A.A. Ramezani pour<sup>1</sup>, M.E. Kamel<sup>2</sup>, A. Kazemian\*<sup>3</sup>, E. Ghasvand<sup>3</sup>,  
H. Shokrani<sup>3</sup> and N. Bakhshi<sup>3</sup>

<sup>1</sup>Concrete Technology and Durability Research Center, Amirkabir University of Technology, Tehran, Iran

<sup>2</sup>Department of Civil Engineering, College of Engineering, University of Tehran, Tehran, Iran

<sup>3</sup>Department of Civil Engineering, Amirkabir University of Technology, Tehran, Iran

(Received March 1, 2012, Revised May 19, 2012, Accepted June 2, 2012)

**Abstract.** This paper presents the results of an investigation on the compressive strength and weight loss of mortars containing three types of fillers as cement replacements; Limestone Filler (LF), Silica Fume (SF) and Trass (TR), subjected to elevated temperatures including 400°C, 600°C, 800°C and 1000°C. Results indicate that addition of TR to blended cements, compared to SF addition, leads to higher compressive strength and lower weight loss at elevated temperatures. In order to model the influence of the different parameters on the compressive strength and the weight loss of specimens, artificial neural networks (ANNs) were adopted. Different diagrams were plotted based on the predictions of the most accurate networks to study the effects of temperature, different fillers and cement content on the target properties. In addition to the impressive RMSE and  $R^2$  values of the best networks, the data used as the input for the prediction plots were chosen within the range of the data introduced to the networks in the training phase. Therefore, the prediction plots could be considered reliable to perform the parametric study.

**Keywords:** blended cement mortars; elevated temperature; limestone; silica fume; trass; compressive strength; weight loss; artificial neural network.

---

## 1. Introduction

Exposing concrete to elevated temperatures causes the mixtures water to evaporate which leads to high pore pressure in the hardened cement paste. This pressure is a function of temperature, heating rate, size of the specimens and porosity. The initial cracks occur around the  $\text{Ca}(\text{OH})_2$  crystals and then progress to areas near the unhydrated cement grains, as supported by Scanning Electron Microscopy (SEM) observations (Piasta 1984). Cracking increases significantly as the temperature is raised beyond 300°C (Piasta 1984, Riley 1991). When the temperature is maintained below 300°C, concrete damage is mostly dominated by localized boundary cracking between the aggregates and the cement paste (Anwar Hossain 2006). Cracks could extend while the concrete is in the post-cooling period (Petzold and Rohr 1970).

Therefore, a reduction of  $\text{Ca}(\text{OH})_2$  content in the cement paste containing supplementary cementing materials (such as SF and TR), which occurs due to the pozzolanic reactions, could help reducing

---

\* Corresponding author, M.Sc student, E-mail: [ak\\_civil85@hotmail.com](mailto:ak_civil85@hotmail.com)

the post-cooling cracks. This fact illustrates the importance of scrutinizing the effect of different mineral additives on cement paste behavior at elevated temperature. At temperatures above 500°C which cause  $\text{Ca}(\text{OH})_2$  disassociation, most concretes lose their main properties including compressive strength (Anwar Hossain 2006).

Many researchers have studied the effect of adding different materials on the compressive strength of mortars (Aydın 2008, Cülfic and Özturan 2002, Aydın and Baradan 2007) and concretes (Poon *et al.* 2004, Demirel and Keleştemur 2010, Xiaoa and Falkner 2006) at elevated temperatures. Yuzer *et al.* (2011) have studied ordinary and pozzolan incorporated mortar samples exposed to elevated temperatures up to 1200°C. They have developed neural networks to model the non-linear relationship among the three factor including color (hue, lightness and chroma), ultrasonic pulse velocity and the compressive strength of mortars and succeeded to predict the compressive strength value with high accuracy using the color parameters and the pulse velocity.

In the present study the effect of replacing cement by Silica fume, Limestone filler and Trass at different levels on mortars subjected to elevated temperatures is investigated. Furthermore, two ANN models are developed for the prediction of compressive strength and weight loss of mortars containing blended cements at temperature up to 1000°C. Based on these models and their predictions, a study on different parameters is conducted.

## 2. Experimental program

### 2.1 Materials

Cement used in the mixtures was ASTM C150 type I Portland cement. Chemical and physical characteristics of Cement (C), Trass (TR), Silica fume (SF) and Limestone filler (LF) are shown in Table 1.

According to the EN 197-1, LF should satisfy these conditions:

(1)  $\text{CaCO}_3$  content higher than 75%, (2) clay content assessed by Methylene blue test (MBA), less than 1.20 g/100 g and (3) the total organic carbon (TOC) content shall conform to one of the following criteria:

–LL: shall not exceed 0.20% by mass

–L: shall not exceed 0.50% by mass

According to Table 1 the local LF satisfies all the mentioned conditions.

### 2.2 Mix designs

A total of 24 different mixtures were prepared and various contents of LF, SF and TR were used. All the mixtures were prepared in accordance with ASTM C109. Mix design proportions are given in Table 2. CL1 to CL8 mixtures contain cement and LF, CLS1 to CLS8 mixtures contain cement, LF and SF, while CLT1 to CLT8 mixtures contain cement, LF and TR at different replacement levels.

Table 1 Composition of materials

Chemical components	Cement	Trass	Silica fume	Limestone filler
Silicon dioxide (SiO <sub>2</sub> ) (%)	21.5	65.74	98	1.47
Aluminum oxide (Al <sub>2</sub> O <sub>3</sub> ) (%)	3.68	12.24	0.2	0.22
Ferric oxide (Fe <sub>2</sub> O <sub>3</sub> ) (%)	2.76	2.05	0.2	0.29
Calcium oxide (CaO) (%)	61.5	2.87	0.1	54.77
Magnesium oxide (MgO) (%)	4.80	0.96	0.1	0.30
Sulphate oxide (SO <sub>3</sub> ) (%)	2.50	-	-	0.06
Sodium oxide (Na <sub>2</sub> O) (%)	0.12	1.92	-	0.05
Potassium oxide (K <sub>2</sub> O) (%)	0.95	2.02	-	0.08
Titanium oxide (TiO <sub>2</sub> ) (%)	0.04	0.29	-	0.05
Manganese oxide (MnO) (%)	0.17	0.02	-	-
Phosphorus oxide (P <sub>2</sub> O <sub>5</sub> ) (%)	0.23	0.03	-	0.01
LOI (%)	1.35	8.50	-	42.23
Physical characteristics				
Blaine (m <sup>2</sup> /kg)	330	350	2000	330
Specific gravity	3.18	2.5		2.69
Chemical Characteristics				
CaCO <sub>3</sub> content (%)	-	-	-	97.8
Total organic carbon (TOC) (%)	-	-	-	0.05
Methylene blue adsorption (MBA) (gr/100 gr)	-	-	-	0.07
Moisture content (%)	-	-	-	0.37
Mineralogical composition				
C <sub>3</sub> S (%)	51	-	-	-
C <sub>2</sub> S (%)	23	-	-	-
C <sub>3</sub> A (%)	5	-	-	-
C <sub>4</sub> AF (%)	8	-	-	-

### 2.3 Preparation of specimens and tests

The testing procedure included the mixing, casting and testing of 50 mm cubes of each mixture. After 24 hours, the cubes were cured in 23°C lime-saturated water until the test age to prevent losing Ca(OH)<sub>2</sub>. Then the specimen's compressive strength and weight loss were measured at the age of 28 days. At this age, specimens were placed in an electrical furnace with heat applied at the rate of 2.5 (°C/min) up to the desired temperature. Three cubes were dried to reach a constant mass before being exposed to elevated temperatures so they can be used as reference for weight loss calculation. A maximum temperature of 400, 600, 800 and 1000°C was maintained for 2 hours.

The specimens were removed and tested after the furnace cooled down to room temperature. Control tests were also performed on specimens cured at room temperature (23°C). Residual compressive strength and weight loss were determined as the mean value of three cubes tested at each temperature.

Table 2 Mix proportions of mortars

Mix ID	Trass (%)	Silica fume (%)	Limestone fume (%)	Cement (%)
CL1	0	0	0	100
CL2	0	0	2.5	97.5
CL3	0	0	5	95
CL4	0	0	7.5	92.5
CL5	0	0	10	90
CL6	0	0	15	85
CL7	0	0	20	80
CL8	0	0	30	70
CLS1	0	5	0	95
CLS2	0	5	10	85
CLS3	0	5	20	75
CLS4	0	5	30	65
CLS5	0	10	0	90
CLS6	0	10	10	80
CLS7	0	10	20	70
CLS8	0	10	30	60
CLT1	5	0	0	95
CLT2	5	0	10	85
CLT3	5	0	20	75
CLT4	5	0	30	65
CLT5	10	0	0	90
CLT6	10	0	10	80
CLT7	10	0	20	70
CLT8	10	0	30	60

### 3. Results and discussion

#### 3.1 Compressive strength

Changes in mechanical properties occur when mortars are subjected to elevated temperatures and the involved mechanisms are quite complex. This is due to the coincidence of chemical and physical changes in hardened cement paste, aggregate and at the interfaces.

Figs. 1-3 demonstrate the residual compressive strength for all mixtures at the age of 28 days. In Fig. 1, which demonstrates CL mixtures behavior at different temperatures, it is observed that up to 200°C, increase in LF content results in compressive strength reduction. The LF increase causes a cement content reduction and consequently an increase in the effective  $w/c$  ratio happens (Ramezaniapour *et al.* 2009). At temperatures around 400°C, an increase in LF replacement level up to 5% (CL1 and CL2) results in a slight increase in compressive strength while more replacement levels cause a slight decrease compared to room temperature. Up to 600°C, increasing

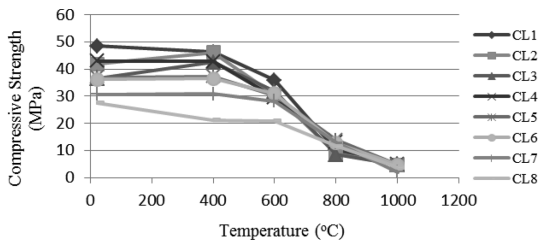


Fig. 1 Compressive strength of CL mixtures (28 days)

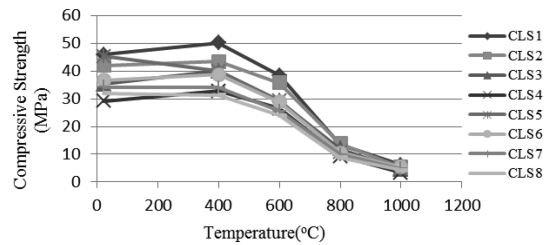


Fig. 2 Compressive strength of CLS mixtures (28 days)

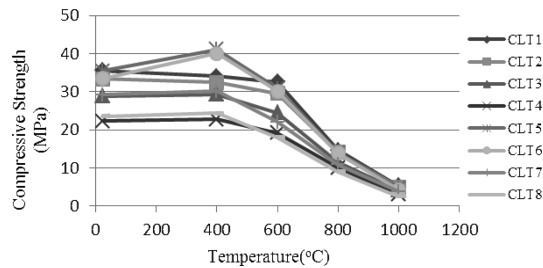


Fig. 3 Compressive strength of CLT mixtures (28 days)

LF replacement level diminishes the compressive strength decrease rate. At temperatures higher than 400°C sudden drop in compressive strength is observed specially in the range of 600°C to 800°C. At temperatures higher than 800°C, compressive strength is decreased approximately with the same constant rate in all mixtures.

Fig. 2 illustrates that CLS mixtures containing LF and 5% of SF (CLS1 to CLS4) show a slight increase in their residual compressive strength up to 400°C while mixtures containing 10% of SF (CLS5 to CLS8) show no significant change in compressive strength. At temperatures higher than 400°C, a drop in residual compressive strength is observed for all mixtures. At temperatures exceeding 800°C, the strength pattern of all mixtures is approximately the same.

According to Fig. 3, subjecting CLT mixtures containing LF and TR to elevated temperatures up to 400°C causes no significant change or even a slight decrease in residual compressive strength is observed except for CLT5 and CLT6 mixtures. Exceeding 400°C all mixtures have sudden drop in residual compressive strength. The highest rate occurs in temperatures between 600°C and 800°C. Exceeding the temperature of 800°C, the behavior of all mixtures is similar.

Rising the temperature up to 200°C, drying and hardening of the surface layer occurs which leads to a small increase in compressive strength. Evaporation of free water in hardened cement paste could be a reason for compressive strength increase (Khoury 1999, Dias *et al.* 1990). Hydration progress of unhydrated cementitious materials could be another cause of the strength increase in hardened cement paste (Khoury 1999). At temperatures higher than 400°C, internal cracking and chemical decomposition of the surface layer occurs which leads to a significant reduction in compressive strength. Micro-cracks occurring in cement paste could be the result of the swelling of physically bound water and thermal incompatibility between aggregates and cement paste (Malhotra 1956). These micro-cracks are responsible for further durability loss in specimens heated to 450, 600 and 800°C (Riley 1991, Lin *et al.* 1996).

At room temperature the average compressive strength of CL1, CL5, CL7 and CL8 mixtures,

which contain 0%, 10%, 20% and 30% of LF respectively, shows approximately 5% increase after replacing 5% and 10% of cement by SF. The same comparison to CLT mixtures reveals that approximately 16% decrease has occurred in compressive strength for both 5% and 10% of TR replacement.

At temperatures up to 400°C, TR content of 10% results in 12% increase in compressive strength, while 5% of TR replacement causes 2% decrease. At temperatures from 400°C to 1000°C, both TR contents of 5% and 10% result in similar compressive strength loss. At 1000°C loss of compressive strength is about 86%, compared to room temperature. The same value is observed for mixtures simply containing same amounts of LF.

At temperatures up to 400°C, 10% SF replacement results in 4% decrease in compressive strength, while 5% of SF replacement causes 10% increase. Up to 600°C, SF contents of 5% and 10% result in 14% and 28% strength loss, respectively. At 1000°C strength loss is about 87%, compared to room temperature.

### 3.2 Weight Loss

Figs. 4-6 show weight loss values at the age of 28 days for all mixtures at various temperatures. At temperatures lower than 400°C, CL mixtures have up to 3% weight loss while CLS and CLT mixtures show up to 8% loss. Weight loss occurring in temperatures of up to 200°C corresponds to the loss of the evaporable water and part of the physically bound water (Bazant and Kaplan 1996). From 200°C to 600°C, the weight loss includes the loss of chemically bound water resulted by decomposition of the C-S-H (Bazant and Kaplan 1996). Exceeding the temperature of 600°C, further weight loss was observed in all samples and this is due to the decomposition of LF, releasing carbon dioxide (Ye *et al.* 2007). Bazant *et al.* (1996) reported that from 110°C to 700°C, the weight loss indicates the loss of chemically bound water caused by decomposition of the C-S-H,

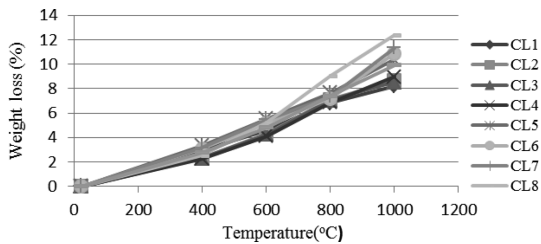


Fig. 4 Weight loss of CL mixtures at different temperatures (28 days)

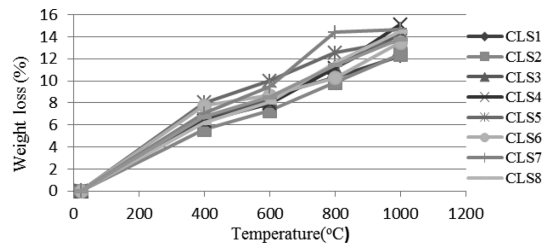


Fig. 5 Weight loss of CLS mixtures at different temperatures (28 days)

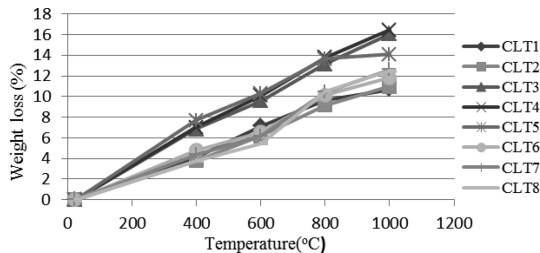


Fig. 6 Weight loss of CLT mixtures at different temperatures (28 days)

the carboaluminate hydrates and the dehydroxylation of CH. When the temperature is higher than 700°C, serious loss of weight has been observed which could be caused by decomposition of carboniferous LF, i.e.,  $\text{CaCO}_3 \rightarrow \text{CaO} + \text{CO}_2$ .

The average weight loss rate in specimens with 5% and 10% SF replacement is approximately 21% and 24% higher than specimens with no SF, respectively. The same contents of TR replacement results in about a 21% and 17% increase in the weight loss rate.

## 4. Application of ANN

### 4.1 ANN methodology

Artificial neural networks are algorithms which are developed to simulate the biological system of the brain. The ANNs can develop input-output complex mappings through a ‘learning process’. This ability, which does not require much information regarding the nature of inputs and outputs, could be the main reason for great popularity of ANNs in modeling complex materials behavior.

Multi-layer feed-forward neural networks are among the most popular which have been used for predicting concrete and mortar behavior by many authors (Demir 2008, Kewalramani and Gupta 2006, Jeyasehar and Sumangala 2006).

Each neuron in a network is connected to some other neurons and a signal is transmitted to it through this connection. In fact, each connection includes a varying weight number which demonstrates the importance of the influence between the connected neurons (Ji *et al.* 2006). Then the neuron calculates the weighted sum of the received inputs and using an activation function, the neuron output is obtained. By reiteration of this process, the data flow continues layer by layer (Demir 2008).

Three types of layers can be defined in a neural network, namely input layer, hidden layer and output layer. The input layer contains the most important parameters affecting the output and no calculations are performed in this layer. The computations are carried out in hidden layers, which may contain many computational units, in order to acquire complex interactions among input/output variables in a problem. Finally, the output layer is where the predicted output by a neural network is obtained. Fig. 7 illustrates a sample neural network which contains one hidden layer.

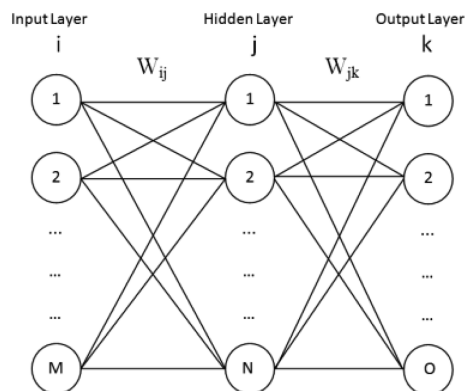


Fig. 7 A sample neural network structure

The back-propagation model is the most common learning system in artificial neural networks. The Levenberg-Marquardt algorithm, which is utilized in this research, both simplifies the learning process in the back-propagation neural network and also decreases the time needed for the training phase (Ji *et al.* 2006).

More details on the learning process and validation and testing phases can be found in (Jeyasehar and Sumangala 2006, Ji *et al.* 2006). The input and output data are normalized within the range of 0 to 1 in a feed-forward network (Demir 2008)

$$X_n = [X - (X)_{\min}] / [(X)_{\max} - (X)_{\min}] \quad (1)$$

Where  $X_n$ ,  $(X)_{\max}$  and  $(X)_{\min}$  are the normalized, maximum and minimum values of data which are given to the network.

## 4.2 Architecture of ANN models

The first step in building an ANN model is determining the model structure. Since there is not any specific rule for determining the best network structure (Kewalramani and Gupta 2006, Lin *et al.* 2003), a trial and error approach was adopted in this study to achieve the best ANN model. Different 3-layer and 4-layer-networks, using common activation functions and different neuron numbers in each layer (1 to 15 neurons in each hidden layer), were developed and processed 100 times. This was done to eliminate the possibility of inappropriate initial weights which are determined randomly. A MATLAB code was developed to run the networks and in this way the most accurate models for predicting the compressive strength and weight loss of mortars containing different fillers were deduced.

Cement, LF, SF and TR content besides temperature are the parameters selected as input for the ANN model. Since the  $W/B$  ratio was kept constant (0.485), this parameter was not considered as an input. The input data were normalized according to Eq. (1). A total of 120 datasets were used for building compressive strength predicting model (CS-ANN), while 96 datasets were available to be used for the weight loss predicting model (WL-ANN). This was due to the omission of 24 datasets obtained by tests in room temperature and used as reference data for weight loss calculations.

In order to determine the best structure for ANN models, coefficient of determination ( $R^2$ ) for the predicted and experimental outputs of the test data was adopted. Test data are unseen by the network during the training phase, hence the predicted output for these data could be a good basis for the evaluation of different networks. According to this criterion, the best networks resulting from a 100 time process are shown in Tables 3 and 4 for the prediction of compressive strength and weight loss, respectively.  $R^2_{\max}$  (test data) is the best coefficient of determination between predicted and experimental outputs for test data and  $R^2_{\max}$  (All) is the best coefficient of determination between predicted and actual outputs for all data (training, validation and test data).

## 4.3 ANN model for the compressive strength prediction (CS-ANN)

### 4.3.1 Best ANN model

As it is shown in Table 3, the best CS-ANN model for mortars containing blended cement is a 4 layer network with 6 neurons in the first hidden layer and 4 neurons in the second one. Hyperbolic tangent sigmoid and Log-sigmoid are identified as proper activation functions to form the most accurate CS-ANN model. RMSE value of 1.69 MPa, between real and predicted values of 120 data,

Table 3 Different networks for the prediction of compressive strength

Functions		Neuron numbers		$R^2_{max}$ (Test data)	$R^2_{max}$ (All)
Tan	Tan	5	5	0.913936	0.984262
Tan	Log	6	4	0.985056	0.985255
Tan	Pur	9	9	0.98109	0.985453
Log	Log	10	3	0.982676	0.986446
Log	Pur	15	5	0.980298	0.981288
Log	Tan	9	1	0.980892	0.988036
Pur	Log	8	7	0.981486	0.985453
Pur	Tan	7	7	0.979704	0.983469
Pur	Pur	10	4	0.758989	0.760907
Pur		5		0.756726	0.761605
Tan		12		0.977132	0.982081
Log		7		0.973774	0.981883

was calculated for this network; which approves the model reliability for predicting compressive strength of blended cement mortars.

#### 4.3.2 Parametric study of the model

In order to investigate the effects of some of the parameters considered as inputs of the best CS-ANN model, a reference mixture is defined. Its composition consists of the average of maximum and minimum amounts of input data (which were introduced to the network before) for each parameter (Table 5). Then, by changing just one of the parameters, different mixtures resulted and their compressive strength could be predicted by the best CS-ANN model identified in the previous section so that the effect of that input could be studied. It should be mentioned that the total cementitious materials of  $500 \text{ kg/m}^3$  were kept constant so changes in the fillers contents were counterbalanced by cement content. On the other hand, when changing the cement content, the difference was distributed among fillers according to their proportions in the reference mixture.

When defining the reference mixture, it was decided to consider the trass content equal to zero. This is due to the lack of data on mixtures containing TR and other fillers simultaneously, which results in the ANN model's inability to predict the compressive strength of mortars containing different contents of both trass and any other filler.

Prediction plots for studying effects of temperature, fillers content and cement content on mortar's

Table 4 Reference mixture

Input	Min	Max	Reference mixture
$T$ content ( $\text{kg/m}^3$ )	0	50	0
Temperature ( $^{\circ}\text{C}$ )	23	1000	510
SF content ( $\text{kg/m}^3$ )	0	50	25
LF content ( $\text{kg/m}^3$ )	0	150	75
Cement content ( $\text{kg/m}^3$ )	300	500	400

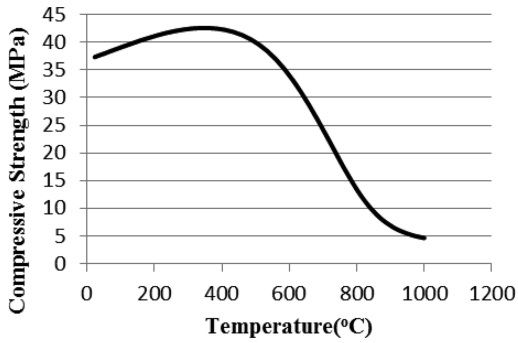


Fig. 8 Effect of elevated temperatures on mortar compressive strength

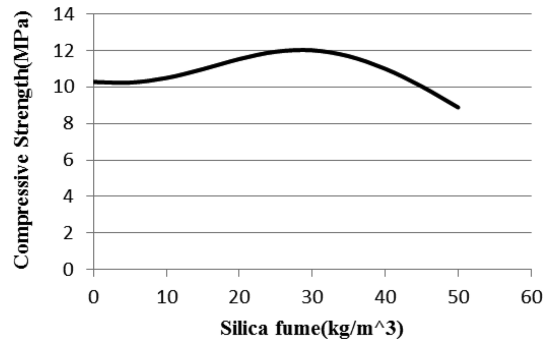


Fig. 9 Effect of SF content on mortar compressive strength at 510°C

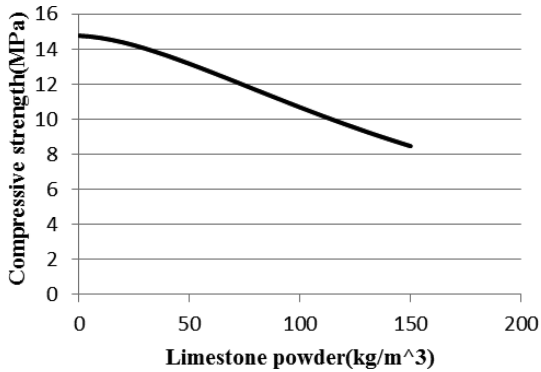


Fig. 10 Effect of LF content on mortar compressive strength at 510°C

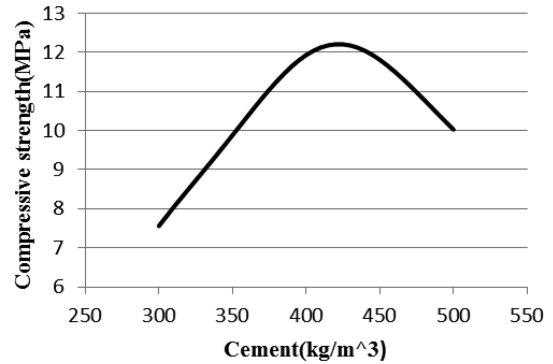


Fig. 11 Effect of cement content on mortar compressive strength at 510°C

compressive strength are presented in Figs. 8-10. These plots could be adopted to find optimum amounts of different materials, investigate the performance of mixtures containing contents of materials other than the amounts used in the experiments.

According to the Fig. 8, a slight increase in compressive strength happens up to 360°C, which could be explained by the positive effect of temperature on hydration reactions. Exceeding this temperature results in the reduction of compressive strength. This phenomenon can be justified by micro-crack propagation, decomposition of the surface layer and incompatibility of thermal coefficients of sand and cement paste. These occurrences are intensified at such temperatures and result in high rate of compressive strength reduction. Beyond 810°C, the rate of strength loss decreases. This could be explained by a porous matrix full of severe cracks which has negligible residual compressive strength and has trifling components susceptible to temperature.

In high temperatures such as 510°C, the hydrothermal interaction of the silica particles and the liberated lime during hydration reaction is intensified and more secondary C-S-H gel is produced, which in turn leads to higher compressive strength. On the other hand, an increase in SF content leads to lower cement content and liberated lime. The shortage of liberated lime hinders the hydration reactions (Morsy *et al.* 2010).

Therefore, it seems that a combination of these two occurrences determines the behavior of the

mortar. It is shown in Fig. 9 that up to 6% (30 kg/m<sup>3</sup>) of SF replacement and intensification of hydration reactions dominates the strength pattern. In higher contents of SF, due to the hindrance of hydration reactions, the propagation of micro-cracks is the major incident affecting the compressive strength loss.

It is reported that limestone undergoes decarbonation (i.e., CaCO<sub>3</sub> → CaO+CO<sub>2</sub>) at temperatures higher than about 600°C, while the rate of decomposition and the decarbonation temperature are not only dependent on temperature and pressure but also on the content of SiO<sub>2</sub> available in the limestone. The resulting Co<sub>2</sub> leads to an increase of pore pressure and internal stress which accelerates the propagation of micro-cracks and reduction of compressive strength (Ye *et al.* 2007).

In Fig. 10, it is observed that a constant decrease in compressive strength occurs by increasing the LF content up to 30%.

In high temperatures two mechanisms dominate the behavior of the mortar. First is the further hydration of unhydrated cement particles as a result of the internal autoclaving effect (Hosam *et al.* 2011) and the second is the micro-cracks propagation due to the increase of pore pressure and internal stress of the mortar which leads to strength loss.

In Fig. 11 it is observed that there is an optimum cement content of 420 kg/m<sup>3</sup> which leads to maximum compressive strength at 510°C. While in lower contents the first mechanism dominates the compressive strength pattern and in higher amounts the second one has the major effect.

#### 4.4 ANN model for weight loss prediction (WL-ANN)

##### 4.4.1 Best ANN model

As it is shown in Table 4, the best WL-ANN model is a 4 layer network containing 11 neurons in the first hidden layer and 2 neurons in the second one. Hyperbolic tangent sigmoid and linear are determined to be proper activation functions to form the most accurate WL-ANN model. RMSE value of 0.94%, between real and predicted values of 96 data, was calculated for this network;

Table 5 Different networks for the prediction of weight loss

Functions		Neuron numbers		R <sup>2</sup> <sub>max</sub> (test data)	R <sup>2</sup> <sub>max</sub> (All)
Tan	Tan	14	5	0.957267	0.935282
Tan	Log	9	9	0.946924	0.92891
Tan	Pur	11	2	0.969634	0.927176
Log	Log	14	8	0.954138	0.954138
Log	Pur	13	5	0.96138	0.918914
Log	Tan	5	4	0.952771	0.963931
Pur	Tan	13	8	0.962361	0.93993
Pur	Log	13	5	0.952771	0.943424
Pur	Pur	9	6	0.826281	0.750302
Pur		14		0.827554	0.753771
Tan		13		0.939736	0.932963
Log		12		0.9409	0.935476

which approves the model reliability for predicting weight loss of blended cement mortar specimens.

**4.4.2 Parametric study of the model**

Similar to the previous section, in order to investigate the effect of inputs on mortar weight loss, a reference mixture was assumed. In this mixture, 700°C is applied as the temperature instead of 510°C which was considered in the previous reference mixture. This is because of the different dataset which does not include the room temperature. The other input amounts are the same as before.

In Fig. 12 it is observed that weight loss increase is approximately proportional to temperature variations. By raising the temperature from 400°C to 1000°C, the weight loss percentage increases from 6% to 15%. This could be explained by the mechanisms described in Section 3.2.

Fig. 13 illustrates the effect of SF content on reference mixture weight loss at 700°C. It is observed that by increasing SF content, the rate of weight loss slows down. According to the explanations in Section 3.2 the major cause of weight loss is the decomposition of the hydration products. It seems that replacing cement by SF leads to lower concentrations of these components; therefore lower rate of weight loss is expected at higher replacement levels.

Fig. 14 shows that changes in LF content result in a maximum change of 1% in weight loss which is in agreement with experimental data presented in Fig. 5, considering the temperature (700°C). According to the explanations in Section 3.2, it seems that decomposition of carboniferous

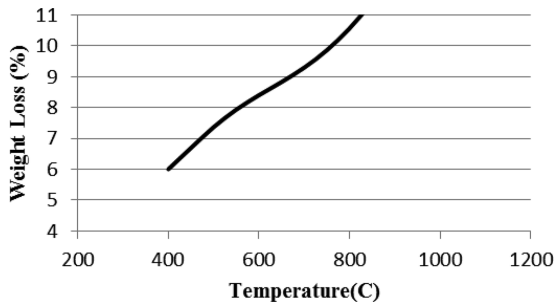


Fig. 12 Effect of elevated temperatures on weight loss of mortar

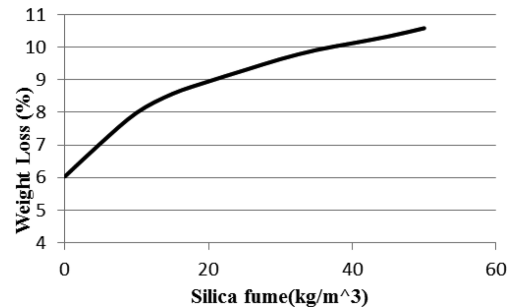


Fig. 13 Effect of SF content on weight loss of mortar at 700°C

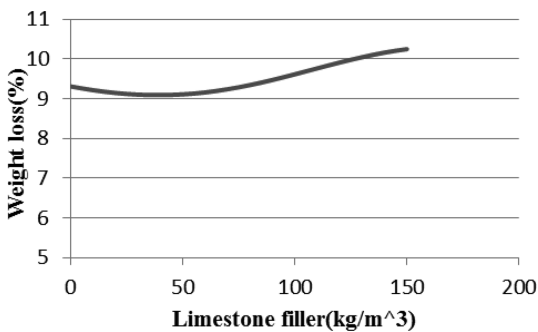


Fig. 14 Effect of LF content on weight loss of mortar at 700°C

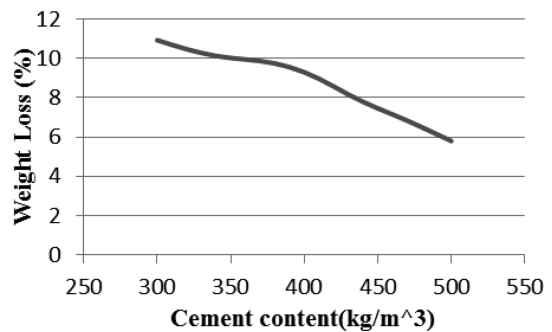


Fig. 15 Effect of cement content on weight loss of mortar at 700°C

LF could be responsible for weight loss. Addition of LF contents higher than 10% seems to intensify this phenomenon and dominate the mortar weight loss pattern.

Fig. 15 implies that increasing cement content causes reduction of weight loss at approximately a constant rate. Change in cement content from  $300 \text{ kg/m}^3$  to  $500 \text{ kg/m}^3$  is expected to cause a 5% variation in weight loss. As discussed previously, decomposition of carboniferous LF and dehydration of the hydration products are the two main phenomena responsible for the weight loss. As long as increase in cement content involves decrease in LF content, it seems that decomposition of carboniferous LF mainly influences weight loss pattern.

## 5. Conclusions

According to the experimental observations and the ANN models developed in this study, the major results are as follows:

1. Up to  $400^\circ\text{C}$ , a slight variation in the residual compressive strength is observed. At temperatures from  $400^\circ\text{C}$  to  $800^\circ\text{C}$ , neglecting the filler type, there is a serious drop in the compressive strength and at temperatures beyond  $800^\circ\text{C}$  similar rate of the compressive strength reduction is occurred in all mixtures. At  $1000^\circ\text{C}$  compressive strength was totally lost.
2. At  $600^\circ\text{C}$ , addition of TR results in the average loss of 14% of initial compressive strength, while this value is 21% for mortars containing SF. At  $800^\circ\text{C}$ , the average loss of 60% is observed for mortars containing TR, while this value reaches 70% for mortars containing SF.
3. Considering weight loss average values at different temperatures, it can be inferred that CL mixtures show superior performance compared to CLS and CLT mixtures. There is not a significant difference between CLS and CLT mixtures performance regarding weight loss. At  $1000^\circ\text{C}$ , the CL mixtures show an average of 10% loss compared to room temperature weight. This value is about 13% for CLS and CLT mixtures.
4. Low RMSE values and high coefficient of determination values of 0.985, 0.970 were obtained by CS-ANN and WL-ANN models, respectively. This high precision approves that ANN models could be applied for the prediction of mortars properties containing blended cements.
5. A parametric study of reference mixture by the best CS-ANN model reveals that optimum contents of SF and cement at  $510^\circ\text{C}$  are 30 and  $420 \text{ kg/m}^3$ , respectively. Furthermore, the LF plot resulting from the CS-ANN model shows that increasing the LF replacement level up to 30% causes 53% loss of compressive strength.
6. A parametric study of the reference mixture by the best WL-ANN model in  $700^\circ\text{C}$  reveals that addition of SF and LF up to 10% and 30%, results in about 5% and 1% of variations in weight loss. It shows higher sensitivity of weight loss to the SF content compared to the LF content.
7. Results show that there is an agreement between ANN plots and experimental results, approving the ANN's satisfactory performance. Therefore, it seems that  $R^2_{\text{max}}(\text{test})$  and RMSE could be adopted as criteria to select the best networks.

## References

- Alaa M. Rashad and Elsokary, T. (2011), "Effect of elevated temperature on physico-mechanical properties of blended cement concrete", *Constr. Build Mater.*, **25**(2), 1009-1017.

- Anwar Hossain, K. (2006), "Macro and microstructural investigations on strength and durability of pumice concrete at high temperature", *J. Mater. Civil Eng.*, **18**(4), 527-536.
- Aydın, S. (2008), "Development of a high-temperature-resistant mortar by using slag and pumice", *Fire Safety J.*, **43**(8), 610-617.
- Aydın, S. and Baradan, B. (2007), "Effect of pumice and fly ash incorporation on high temperature resistance of cement based mortars", *Cement Concrete Res.*, **37**(6), 988-995.
- Bazant, Z.P. and Kaplan, M.F. (1996), *Concrete at high temperatures: Material properties and mathematical models*, London, UK: Longman.
- Bazant, Z.P. and Kaplan, M.F. (1996), *Concrete at high temperatures*, Longman Addison-Wesley, London.
- Cülfic, M.S. and Özturan, T. (2002), "Effect of elevated temperatures on the residual mechanical properties of high-performance mortar", *Cement Concrete Res.*, **32**(5), 809-816.
- Demir, F. (2008), "Prediction of elastic modulus of normal and high strength concrete by artificial neural networks", *Constr. Build Mater.*, **22**(7), 1428-1435.
- Demirel, B. and Keleştemur, O. (2010), "Effect of elevated temperature on the mechanical properties of concrete produced with nely ground pumice and silica fume", *Fire Safety J.*, **45**(6-8), 385-391.
- Dias, D.P.S., Khoury, G.A. and Sullivan, P.J.E. (1990), "Mechanical properties of hardened cement paste exposed to temperatures up to 700°C (1,292°F)", *ACI Mater. J.*, **87**(2), 160-165.
- Jeyasehar, C.A. and Sumangala, K. (2006), "Damage assessment of prestressed concrete beams using artificial neural network (ANN) approach", *Comput. Struct.*, **84**(26-27), 1709-1718.
- Ji, T., Lin, T. and Lin, X. (2006), "A concrete mix proportion design algorithm based on artificial neural networks", *Cement. Concrete Res.*, **36**(7), 1399-1408.
- Kewalramani, M.A. and Gupta, R. (2006), "Concrete compressive strength prediction using ultrasonic pulse velocity through artificial neural networks", *Automat Constr.*, **15**(3), 374-379.
- Khoury, G.A. (1999), "Compressive strength of concrete at high temperatures: A reassessment", *Mag. Concrete Res.*, **44**(161), 291-309.
- Lin, W.M., Lin, T.D. and Powers-Couche, L.J. (1996), "Microstructures of fire-damaged concrete", *ACI Mater. J.*, **93**(3), 199-205.
- Lin, Y., Lai, C.P. and Yen, T. (2003), "Prediction of ultrasonic pulse velocity (UPV) in concrete", *ACI Mater. J.*, **100**(1), 21-28.
- Malhotra, H.L. (1956), "Effect of temperature on the compressive strength of concrete", *Mag. Concrete Res.*, **8**(23), 85-94.
- Morsy, M.S., Alsayed, S.H. and Aqel, M. (2010), "Effect of elevated temperature on mechanical properties and microstructure of silica flour concrete", *IJCEE.*, **10**(1), 1-6.
- Petzold, A. and Rohr, M. (1970), *Concrete for high temperatures*, london, UK: Maclaren and Sons, 232.
- Piasta, J. (1984), "Heat deformations of cement phases and the microstructure of cement paste", *Mater. Struct.*, **17**(102), 415-420.
- Poon, C.S., Shui, Z.H. and Lam, L. (2004), "Compressive behavior of fiber reinforced high-performance concrete subjected to elevated temperatures", *Cement Concrete Res.*, **34**(12), 2215-2222.
- Ramezani pour, A.A., Ghiasvand, E., Nickseresht, I., Mahdikhani, M. and Moodi, F. (2009), "Influence of various amounts of limestone powder on performance of Portland limestone cement concretes", *Cement Concrete Comp.*, **31**(10), 715-720.
- Riley, M.A. (1991), "Possible new method for assessment of fire damaged concrete", *Mag. Concrete Res.*, **43**(155), 87-92.
- Xiaoa, J. and Falkner, H. (2006), "On residual strength of high-performance concrete with and without polypropylene bres at elevated temperatures", *Fire Safety J.*, **41**(2), 115-121.
- Ye, G., Liu, X., De Schutter, G., Taerwe, L. and Vandeveldel, P. (2007), "Phase distribution and microstructural changes of self-consolidating cement paste at elevated temperature", *Cement Concrete Res.*, **37**(6), 978-987.
- Yuzer, N., Akbas, B. and Kizilkanat, A.B. (2011), "Predicting the high temperature effect on mortar compressive strength by neural network", *Comput. Concrete*, **8**(5), 491-511.